

# PHYSICAL REVIEW B

## SOLID STATE

THIRD SERIES, VOL. 1, No. 11

1 JUNE 1970

### Nuclear Quadrupole Coupling and Crystal-Field Effects in the Cubic Intermetallic Compounds $\text{ErAl}_3$ , $\text{TmAl}_3$ , and $\text{YbAl}_3$

H. W. de Wijn\* and A. M. van Diepen†

*Natuurkundig Laboratorium der Universiteit van Amsterdam, ‡ Amsterdam, The Netherlands*

and

K. H. J. Buschow

*Philips Research Laboratories, Eindhoven, The Netherlands*

(Received 6 February 1970)

The presence of a large nuclear quadrupole coupling of the Al nucleus, as measured with NMR, in the cubic rare-earth aluminum intermetallic compounds  $\beta\text{-ErAl}_3$ ,  $\text{TmAl}_3$ , and  $\text{YbAl}_3$  indicates that the net charges at the rare-earth and aluminum sites differ by as much as 3 to 4 unit charges. Data on the magnetic susceptibility and this result have been used to analyze crystal-field effects in  $\text{TmAl}_3$ . The ground state appears to be a nonmagnetic doublet  $\Gamma_3$ , the next higher level being the triplet  $\Gamma_5^{(1)}$  at a distance of 45°K. In addition, from the Knight shift, exchange constants between conduction electrons and 4f electrons have been derived to be  $\mathcal{J}_{sf} = -0.24$  eV.

#### I. INTRODUCTION

The intermetallic compounds  $\beta\text{-ErAl}_3$ ,  $\text{TmAl}_3$ , and  $\text{YbAl}_3$  have the cubic  $\text{Cu}_3\text{Au}$  structure.<sup>1</sup> The rare-earth ions are located at the corners of a cube, while the aluminum ions are at the centers of the faces. The point symmetry at the rare-earth site is essentially cubic.

The nature of the crystal field at the rare-earth site may well be discussed in terms of the point-charge model. The point charges, positioned at the lattice sites, do not merely represent the effective charges of the ions, as in insulators, but, to the extent that the conduction-electron charge densities are radial about the lattice positions, also the spatial distribution of the conduction electrons. From measurements of the magnetic susceptibility of  $\text{CeAl}_2$ , White *et al.*<sup>2</sup> concluded that in the metallic rare-earth aluminides the aluminum is negatively charged and the rare earth positively. In Sec. II further and direct evidence for this conclusion is presented by examining the nuclear quadrupole coupling of the Al nucleus in the cubic  $\text{RAl}_3$  compounds, which for this particular lattice struc-

ture is directly related to the charge difference between rare-earth and aluminum sites.

From the magnetic point of view, the most interesting of the compounds is  $\text{TmAl}_3$ . The free  $\text{Tm}^{3+}$  ion has an integral  $J$  ground-state multiplet ( $J = 6$ ), and in this case the crystal-field splitting usually leaves a Van Vleck-type state as the ground state. That is to say, the moment induced by an external magnetic field and/or exchange field arises exclusively from admixtures of the wave functions of excited crystal-field states into the wave functions of the crystal-field ground state, whereas no moment is induced by redistribution of the ions over the Zeeman states of the crystal-field ground state. This situation occurs if the ground state is a singlet. For the intermetallic compound  $\text{TmSb}$ , for example, where, as in  $\text{TmAl}_3$ , the Tm ion is at a site of cubic symmetry, Cooper and Vogt<sup>3</sup> have recently demonstrated unambiguously that the singlet  $\Gamma_1$  is the ground state by analyzing the magnetic susceptibility and anisotropic magnetization of a single crystal. It is less well known that pure Van Vleck paramagnetism of  $\text{Tm}^{3+}$  will also occur in the case where the crystal-field ground state is

the doublet  $\Gamma_3$ . The sublevels of  $\Gamma_3$  do not have a magnetic moment, and therefore do not show Curie paramagnetism. In Sec. III, it is shown that the magnetic susceptibility as a function of the temperature and the conclusions arrived at in Sec. II are appropriate for the latter situation to occur in  $\text{TmAl}_3$ .

In addition, in Sec. IV exchange constants between conduction electrons and  $4f$  electrons are derived from the isotropic Knight shift.

## II. NUCLEAR QUADRUPOLE COUPLING AT Al SITE

Nuclear magnetic resonance (NMR) of the  $^{27}\text{Al}$  nucleus ( $I = \frac{5}{2}$ ), observed between 100 and 300 °K with a crossed-coils induction spectrometer at frequencies of 8, 6, and 4 MHz, showed a strong nuclear quadrupole coupling (Table I).

The point symmetry of the Al site being axial, the NMR line of the  $^{27}\text{Al}$  nucleus is split into five transitions. For a powder this results, after averaging over all orientations of the field gradient axis relative to the magnetic field,<sup>4</sup> in a central line ( $m_I = +\frac{1}{2} \leftrightarrow -\frac{1}{2}$ ), unshifted in first order, and four satellites at mutual distances  $3e^2qQ/4I(2I-1)$ . The shape of the central line of the powder spectrum is split in second order, and in addition is affected by anisotropy in the Knight shift. Theoretical line shapes for various ratios of these two effects have been calculated in great detail by Barnes *et al.*<sup>5</sup> In the compounds under study, quadrupole effects appeared to give by far the largest contribution to the splitting of the central line. An estimate of the anisotropic Knight-shift linewidth parameter<sup>5</sup> resulted for  $\text{TmAl}_3$  in  $a \approx 0.005$ , whereas in the other compounds no anisotropy could be detected. Values for  $|e^2qQ|$  were derived from the splitting of the central line, and in some cases also from the spacing between the first-order satellites with results identical within the experimental error. In  $\text{TmAl}_3$ ,  $|e^2qQ|$  increases slightly towards lower temperatures; in the other compounds, it is a constant within the experimental accuracy.

On the basis of the point-charge model, the electric field gradient  $q$  at a site of axial symmetry can be written as

$$q = (1 - \gamma_\infty) \sum_i Z_i (3 \cos^2 \vartheta_i - 1) / r_i^3, \quad (1)$$

where  $Z_i$  is the charge at the ion at  $\vec{r}_i$ ,  $\vartheta_i$  is the angle between the  $q$  axis and  $\vec{r}_i$ , and  $\gamma_\infty$  is the antishielding factor. If the rare-earth and aluminum sites would carry equal point charges, the aluminum would be situated, as far as charges are concerned, at a point of cubic symmetry with a

TABLE I. Nuclear quadrupole coupling constants of the  $^{27}\text{Al}$  nucleus at 300 °K and exchange constants between conduction and  $4f$  electrons in cubic  $R\text{Al}_3$  compounds.

Compound	$ e^2qQ/h $ (MHz)	$J_{sf}$ (eV)
$\beta\text{-ErAl}_3$	$8.3 \pm 0.5$	$-0.24$
$\text{TmAl}_3$	$7.6 \pm 0.2$	$-0.24$
$\text{YbAl}_3$	$7.2 \pm 0.2$	$-0.23$

twelve-fold nearest-neighbor coordination and no electric field gradient would be present. By virtue of this, the experimental  $q$  is directly related to the charge *difference* between the rare-earth and aluminum sites. Using the theoretical value  $\gamma_\infty = -2.36$ ,<sup>6</sup> and the lattice parameter  $a = 4.200 \text{ \AA}$ ,<sup>1</sup> lattice summation with an Al site in the origin over unit charges at the other Al sites in  $\text{TmAl}_3$  results in a total of  $q = +0.393 \times 10^{24} \text{ cm}^{-3}$ ; lattice summation over unit charges at the Tm sites yields  $q = -0.393 \times 10^{24} \text{ cm}^{-3}$ . With the experimental  $|e^2qQ/h| = 7.6 \text{ MHz}$  and  $Q(^{27}\text{Al}) = 0.149 \times 10^{-24} \text{ cm}^2$ ,<sup>7</sup> we have an experimental  $q = 1.41 \times 10^{24} \text{ cm}^{-3}$ , which indicates that the charges at the Al and Tm sites differ by 3.7 unit charges. The experiment gives the absolute value only, but because the electron work function of aluminum is larger than those of the rare-earth metals, it is obvious that the Al ions attract more electrons than the rare-earth ions. Both Al and Tm being trivalent, the upper-limit set for the net charge at an Al or Tm site is  $+3e$ . The observed charge difference therefore indicates that the net charges at the Al and Tm sites are of opposite sign.

The crystal field at the Tm ion, like the electric field gradient at the Al nucleus, is the result of charges at the lattice sites. In Sec. III, we will undertake an analysis of crystal-field effects in  $\text{TmAl}_3$  by using data on the magnetic susceptibility in addition to the results of this section, which may be summarized as follows: The Tm sites carry a *positive* charge, close to  $+3e$ , while the Al sites carry a *negative* charge of about  $-e$ .

## III. CRYSTAL FIELD AT Tm SITE

For the cubic point symmetry at the  $\text{Tm}^{3+}$  ion ( $J = 6$ ), we have the crystal-field Hamiltonian, taking the axis of quantization parallel to one of the cube axes,<sup>8</sup>

$$\mathcal{H}_{\text{cryst}} = B_4 (O_4^0 + 5O_4^4) + B_6 (O_6^0 - 21O_6^4), \quad (2)$$

with

$$O_4^0 = 35J_z^4 - 30J(J+1)J_z^2 + 25J_z^2 - 6J(J+1) + 3J^2(J+1)^2$$

$$\begin{aligned}
 O_4^4 &= \frac{1}{2}(J_+^4 + J_-^4), \\
 O_6^0 &= 231J_z^6 - 315J(J+1)J_z^4 + 735J_z^4 + 105J^2(J+1)^2J_z^2 \\
 &\quad - 525J(J+1)J_z^2 + 294J_z^2 - 5J^3(J+1)^3 \quad (3) \\
 &\quad + 40J^2(J+1)^2 - 60J(J+1),
 \end{aligned}$$

$$\begin{aligned}
 O_6^4 &= \frac{1}{4}\{[11J_z^2 - J(J+1) - 38](J_+^4 + J_-^4) \\
 &\quad + (J_+^4 + J_-^4)[11J_z^2 - J(J+1) - 38]\}.
 \end{aligned}$$

The fourth- and sixth-order crystal-field intensities  $B_4$  and  $B_6$  are usually expressed as<sup>9</sup>

$$\begin{aligned}
 B_4 &= Wx/F_4, \\
 B_6 &= W(1 - |x|)/F_6, \quad |x| \leq 1,
 \end{aligned} \quad (4)$$

where  $x$  is the relative strength of the fourth- and sixth-order crystalline-field potentials and  $W$  is an absolute scaling factor of the over-all crystal-field splitting having the dimension of an energy.  $F_4$  and  $F_6$  are numerical constants specified for a given  $J$  (for  $J=6$ ,  $F_4=60$ , and  $F_6=7560$ ).

The thirteen-fold degenerate ground multiplet of the free  $\text{Tm}^{3+}$  ion is split by the cubic crystal field into two singlets  $\Gamma_1$  and  $\Gamma_2$ , having different symmetry, one doublet  $\Gamma_3$ , and three triplets  $\Gamma_4$ ,  $\Gamma_5^{(1)}$ , and  $\Gamma_5^{(2)}$ , the latter two having identical symmetry properties. Their energies and eigenfunctions have been calculated by diagonalization of the secular determinant of  $\mathcal{H}_{\text{cryst}}$  for various values of  $x$ , and have subsequently been used to calculate the susceptibility as a function of the temperature.

The susceptibility was obtained by introducing the Zeeman energy of the rare-earth ion's magnetic moment in an external applied field  $H$  and an exchange field  $H_{\text{ex}}$ , the latter acting on the spin only, as a perturbation on the crystal-field problem,

$$\mathcal{H}_{\text{pert}} = \mu_B [gH + 2(g-1)H_{\text{ex}}] J_z. \quad (5)$$

We proceed by calculating the expectation values  $\langle J_z \rangle$  and averaging them over the crystal-field levels and their Zeeman sublevels according to the Boltzmann statistics to obtain  $\langle J_z \rangle_{\text{av}}$ , which is linearly proportional to the induced moment, in terms of  $H$  and  $H_{\text{ex}}$ . We retain only terms linear in  $H$  and  $H_{\text{ex}}$ , and in doing so obtain a Curie-type term inversely proportional to the temperature, and a Van Vleck-type term independent of the temperature, as pointed out in Van Vleck's book.<sup>10</sup> That is,

$$\langle J_z \rangle_{\text{av}} = \mu_B [gH + 2(g-1)H_{\text{ex}}]$$

$$\times \sum_m \left( -\frac{|\langle m | J_z | m \rangle|^2}{kT} + 2 \sum_{n \neq m} \frac{|\langle m | J_z | n \rangle|^2}{E_m - E_n} \right) P(m), \quad (6)$$

in which the summations are over the crystal-field levels  $|m\rangle$  with energy  $E_m$  and Boltzmann statistical weight  $P(m)$ . To eliminate  $H_{\text{ex}}$  we substitute its value on the basis of the linear molecular field approximation,

$$2\mu_B H_{\text{ex}} = -g(g-1) \langle J_z \rangle_{\text{av}}, \quad (7)$$

and obtain<sup>11</sup>

$$\begin{aligned}
 \frac{g\mu_B H}{\langle J_z \rangle_{\text{av}}} &= \left[ \sum_m \left( -\frac{|\langle m | J_z | m \rangle|^2}{kT} \right. \right. \\
 &\quad \left. \left. + 2 \sum_{n \neq m} \frac{|\langle m | J_z | n \rangle|^2}{E_m - E_n} \right) P(m) \right]^{-1} + g(g-1)^2, \quad (8)
 \end{aligned}$$

which is proportional to the reciprocal susceptibility, at low fields, through

$$\chi = -Ng\mu_B \langle J_z \rangle_{\text{av}} / H. \quad (9)$$

Figure 1 shows the results of the calculation for  $W > 0$  and  $W < 0$ , and various values of  $x$  in the absence of exchange. According to Eq. (8) the effect of exchange is simply to shift the curves in Fig. 1 in the vertical direction by  $g(g-1)^2/W$ , and that upward for antiferromagnetic exchange. These curves are to be compared with the experimental  $\chi^{-1}$ -versus- $T$  curve (Fig. 2), which follows a Curie-Weiss law above approximately 40°K and becomes temperature independent at low temperatures.<sup>12</sup> In fact, quite a number of theoretical curves can be fitted to the experiment within the experimental accuracy, each of which determines values for  $W$  and  $g$  for a given value of  $x$ . The possible sets of values for  $x$  and  $W$  are collected in Fig. 3 after being converted to the fourth- and sixth-order crystal-field parameters  $A_4 \langle r^4 \rangle = B_4/\beta$  and  $A_6 \langle r^6 \rangle = B_6/\gamma$  by use of Eq. (4) and the Stevens multiplicative factors  $\beta$  and  $\gamma$  (for  $\text{Tm}^{3+}$   $\beta = +8/49005$  and  $\gamma = -5/891891$ ). Within the experimental error,  $g$  turned out to be a constant for all possible combinations, corresponding to a paramagnetic Curie temperature

$$\theta_p = g(g-1)^2 J(J+1)/3k = -6^\circ\text{K}. \quad (10)$$

An answer to the problem which set of values of  $W$  and  $x$  in Fig. 3 constitutes the actual set can be given by means of the point-charge model, which offers a gauge for  $A_4$  and  $A_6$ .<sup>13</sup> A serious handicap of this procedure usually is uncertainty in the signs of the charges at the different lattice sites.<sup>14</sup> In the present case of  $\text{TmAl}_3$  we use the results of

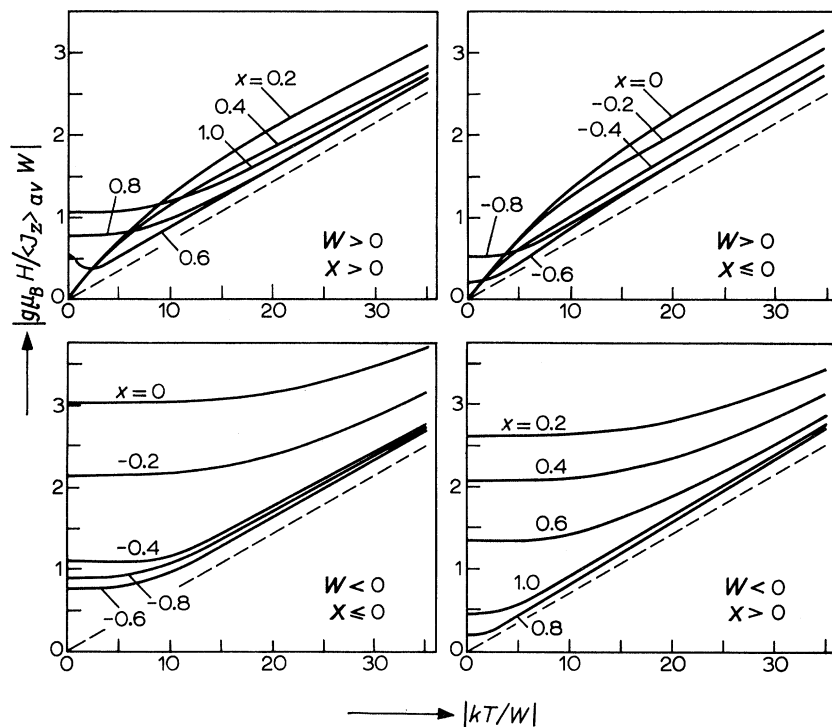


FIG. 1. Calculated values of  $|g\mu_B H / \langle J_z \rangle_{av} W| = N\mu_B^2 g^2 / \chi$  as a function of  $|kT/W|$  for  $J=6$  in the absence of exchange between the ions. The dashed lines, having a slope of  $3/J(J+1)$ , represent the free-ion behavior.

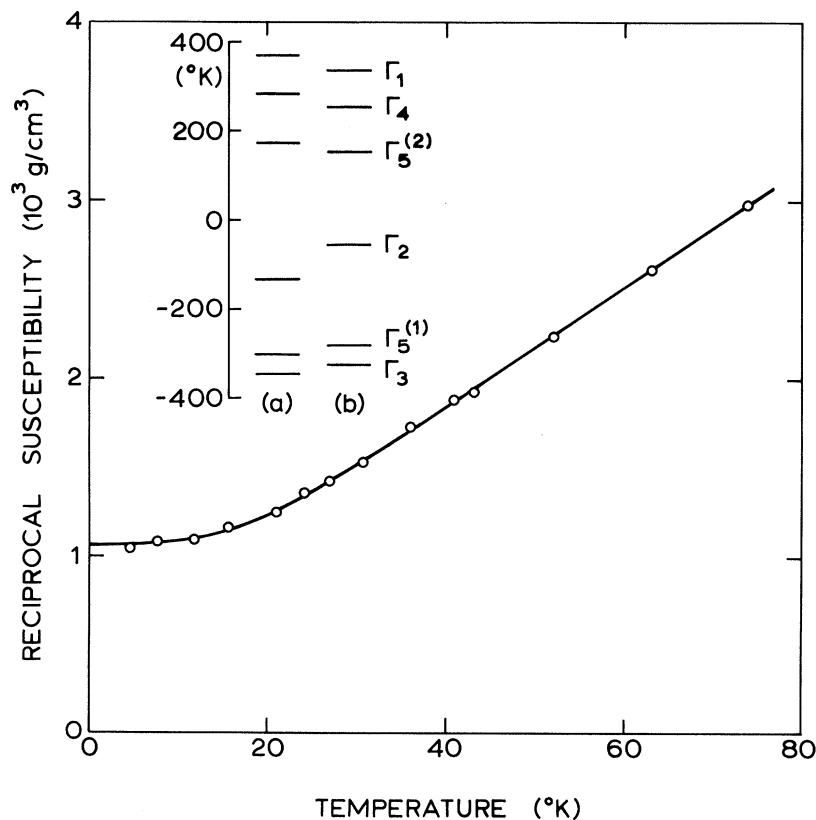


FIG. 2. Experimental reciprocal susceptibility versus the temperature for  $\text{TmAl}_3$ . Insert shows two of the possible level schemes for  $\text{Tm}^{3+}$  in the cubic crystal field in this compound. (a)  $W/k = +3.23^\circ\text{K}$ ,  $x = -0.90$ ; (b)  $W/k = +3.24^\circ\text{K}$ ,  $x = -0.80$ .

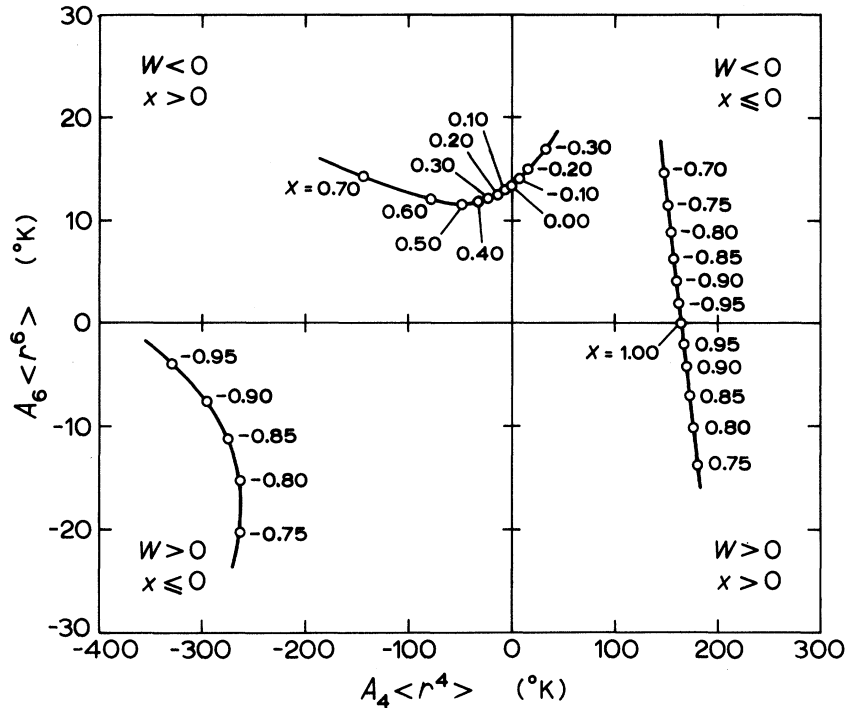


FIG. 3. Crystal-field parameters  $A_4\langle r^4 \rangle = B_4/\beta$  and  $A_6\langle r^6 \rangle = B_6/\gamma$  ( $\beta$  and  $\gamma$  are the Stevens multiplicative factors) for  $\text{Tm}^{3+}$  in  $\text{TmAl}_3$ , as derived from susceptibility data.

Sec. II, representing the Tm and Al sites by  $+3e$  and  $-e$ , respectively. The  $\text{Tm}^{3+}$  has a twelve-fold cubic coordination of nearest-neighbor Al and a sixfold coordination of nearest-neighbor Tm, which produce - the charges at the Al and Tm being opposite - additive contributions to both  $A_4\langle r^4 \rangle$  and  $A_6\langle r^6 \rangle$ . These parameters are found to be negative with a ratio of 25, which implies that  $W$  is positive and  $x$  negative, close to  $-0.85$ . The insert of Fig. 2 shows two possible level schemes. In all cases of the lower left-hand quadrant of Fig. 3, the nonmagnetic doublet  $\Gamma_3$  is the lowest level. The distance to the next level, the triplet  $\Gamma_5^{(1)}$ , as derived from the analysis of the susceptibility, is very much independent of  $x$ , and amounts to  $45^\circ\text{K}$ . For  $\text{Tm}^{3+}$  in  $\text{TmSb}$ , the order of the crystal-field levels is just reversed.<sup>3</sup> Interestingly, also according to the point-charge model the signs of  $A_4$  and  $A_6$  are reversed, since the coordination of  $\text{Tm}^{3+}$  by the first neighbor Tm in  $\text{TmSb}$  is twelve-fold, instead of sixfold as in  $\text{TmAl}_3$ , and the coordination by the nonmagnetic ion sixfold, instead of twelve-fold. The level schemes depicted in Fig. 2 are essentially different from those obtained under the assumption of a positive charge at the Al sites. In the latter case the Van Vleck-type temperature-independent paramagnetism observed for  $\text{TmAl}_3$  below  $20^\circ\text{K}$  would be due to a magnetic singlet rather than a nonmagnetic doublet.

#### IV. $J_{sf}$ EXCHANGE CONSTANTS

In addition, phenomenological exchange constants  $J_{sf}$  of the interaction between conduction electron spins and rare-earth ion spins,  $\mathcal{H} = -J_{sf} \vec{s} \cdot \vec{S}$ , have been derived from the temperature dependence of the isotropic Knight shifts as compared with the susceptibilities (Table I). Both the Knight shift and the susceptibility<sup>12</sup> follow Curie-Weiss behavior in the temperature range in which the Knight shift was observed ( $100$ – $300^\circ\text{K}$ ). The contribution to the Knight shift from magnetic dipole fields<sup>15</sup> of the rare-earth moments is quite substantial, and the  $J_{sf}$  values were derived after the correction for the dipole fields had been applied. The values are close to those derived for the non-cubic  $R\text{Al}_3$  compounds,<sup>16</sup> which have a number of different crystal structures.<sup>1</sup> For  $\beta$ - $\text{ErAl}_3$  and  $\text{TmAl}_3$  an interpretation in terms of the Ruderman-Kittel-Kasuya-Yosida theory leads to the same results as for  $\text{GdAl}_3$ ,<sup>17</sup> primarily because the functions  $\Sigma_R$  and  $\Sigma_{A1}$  calculated in Ref. 17 for the hexagonal compound  $\text{GdAl}_3$  are practically identical to those calculated for the cubic compounds in the present investigation. Also those calculated for the complicated structure of  $\text{HoAl}_3$  are very close to them.  $\text{YbAl}_3$  is a different case because its  $4f^{14}$  level is situated close to the Fermi level. Knight shift and susceptibility are still proportion-

al, but their values are smaller by an order of

magnitude than in, for example,  $\text{TmAl}_3$ .

\*On leave of absence at Bell Telephone Laboratories, Murray Hill, N. J.

†On leave of absence at the Department of Chemistry, University of Pittsburgh, Pittsburgh, Pa.

‡Part of the work performed in Amsterdam has been supported by the Foundations F.O.M. and Z.W.O.

<sup>1</sup>J. H. N. van Vucht and K. H. J. Buschow, *J. Less-Common Metals* **10**, 98 (1966).

<sup>2</sup>J. A. White, H. J. Williams, J. H. Wernick, and R. C. Sherwood, *Phys. Rev.* **131**, 1039 (1963).

<sup>3</sup>B. R. Cooper and O. Vogt, *Phys. Rev.* (to be published).

<sup>4</sup>A. Abragam, *The Principles of Nuclear Magnetism* (Oxford U. P., Oxford, England, 1961).

<sup>5</sup>R. G. Barnes, W. H. Jones, and T. P. Graham, *Phys. Rev. Letters* **6**, 221 (1961); W. H. Jones, T. P. Graham, and R. G. Barnes, *Phys. Rev.* **132**, 1898 (1963).

<sup>6</sup>R. M. Sternheimer, *Phys. Rev.* **146**, 143 (1966).

<sup>7</sup>H. Lew and G. Wessel, *Phys. Rev.* **90**, 1 (1953).

<sup>8</sup>M. T. Hutchings, in *Solid State Physics*, edited by F. Seitz and D. Turnbull (Academic, New York, 1964), Vol. 16, p. 227 ff.

<sup>9</sup>K. R. Lea, M. J. M. Leask, and W. P. Wolf, *J. Phys. Chem. Solids* **23**, 1381 (1962).

<sup>10</sup>J. H. Van Vleck, *The Theory of Electric and Magnetic Susceptibilities* (Oxford U. P., Oxford, England, 1932).

<sup>11</sup>In the derivation of the magnetic field has been chosen to point along one of the cube axes. This is not a restriction because the low-field susceptibility is isotropic.

As a check on our computer programs some of the calculations have been repeated starting from a crystal-field Hamiltonian with the quantization axis parallel to [111].

<sup>12</sup>K. H. J. Buschow and J. F. Fast, *Z. Physik Chem. (Frankfurt)* **50**, 1 (1966).

<sup>13</sup>Although some doubt has been thrown upon this model, it is quite reliable in determining the signs of crystal-field terms. See, for instance, R. J. Elliott, in *Magnetism*, edited by G. T. Rado and H. Suhl (Academic, New York, 1965), Vol. IIA. Also R. J. Birgenau, E. Bucher, L. Passell, D. L. Price, and K. C. Turberfield, *J. Appl. Phys.* (to be published), who give a direct determination of crystal-field levels of  $\text{Pr}^{3+}$  in  $\text{PrBi}$  by use of neutron scattering techniques. More pertaining to the present case is  $\text{Tm}^{3+}$  in  $\text{TmSb}$ , for which the point-charge model is also correct in predicting the signs (Ref. 3 and below).

<sup>14</sup>B. R. Cooper, *Helv. Phys. Acta* (to be published).

<sup>15</sup>A. M. van Diepen, K. H. J. Buschow, and H. W. de Wijn, *J. Chem. Phys.* **51**, 5259 (1969).

<sup>16</sup>A. M. van Diepen, H. W. de Wijn, and K. H. J. Buschow, *J. Chem. Phys.* **46**, 3489 (1967); *Phys. Letters* **26A**, 340 (1968); H. W. de Wijn, A. M. van Diepen, and K. H. J. Buschow, *Phys. Rev.* **161**, 253 (1967).

<sup>17</sup>K. H. J. Buschow, J. F. Fast, A. M. van Diepen, and H. W. de Wijn, *Phys. Status Solidi* **24**, 715 (1967); H. W. de Wijn, K. H. J. Buschow, and A. M. van Diepen, *ibid.* **30**, 759 (1968).

## Cooperative Energy Transfer from $\text{Yb}^{3+}$ to $\text{Tb}^{3+}$ in $\text{YF}_3$

F. W. Ostermayer, Jr., and L. G. Van Uitert

*Bell Telephone Laboratories, Murray Hill, New Jersey 07974*

(Received 21 November 1969)

The transfer of energy from  $\text{Yb}^2F_{5/2}$  to  $\text{Tb}^5D_4$  by the cooperative action of two  $\text{Yb}^{3+}$  ions has been observed in  $\text{YF}_3$ . The correlation between the  $\text{Tb}^5D_4$  intensity and the  $\text{Yb}^2F_{5/2}$  and  $\text{Tb}^5D_4$  lifetimes as a function of Tb concentration supports the conclusion that cooperative transfer has taken place. At an exciting (9300 Å) intensity of  $1 \text{ Wcm}^{-2}$  the emitted  $\text{Tb}^5D_4$  (4900, 5460, 5850, and 6200 Å) power from a thin layer of powdered material was  $0.8 \times 10^{-6} \text{ Wcm}^{-2}$ .

Emission of radiation from the  $\text{Tb}^5D_4$  manifold in  $\text{YF}_3$  doped with  $\text{Yb}^{3+}$  and  $\text{Tb}^{3+}$  has been observed under 9300-Å excitation. Our experiments indicate this is due to two excited Yb ions cooperatively transferring their energy to one Tb ion exciting it from the ground state to the  $^5D_4$  manifold.

Figure 1 shows the emission spectrum of  $\text{Y}_{0.3}\text{Yb}_{0.5}\text{Tb}_{0.2}\text{F}_3$ . The lines at 4900, 5460, 5850, and 6200 Å agree with emissions from  $\text{Tb}^5D_4$  to  $^7F_6$ ,

$^7F_5$ ,  $^7F_4$ , and  $^7F_3$ , respectively. The intensities of these lines vary as the second power of the excitation intensity as shown in Fig. 2 for the 5460-Å line. This indicates that the absorption of two photons by the phosphor is required to raise one Tb ion to the  $^5D_4$  manifold.

As the effect is quite weak, in order to have sufficient excitation intensity and to be sure no shorter wavelengths are present which could excite  $\text{Tb}^5D_4$  directly, we placed the material